Wind energy technology has matured as there is now a good basic understanding of several important aspects of wind turbines for large-scale power generation.

Wind Energy Conversion

J.B. Dragt

Institute for Wind Energy
Delft University of Technology, The Netherlands

Fig. 1 — Propeller-type wind turbines.

Will wind and solar energy provide the ultimate answer to problems of fuel depletion, air pollution and global warming? Perhaps so, although one presumes that there will not be a single answer. But wind energy can certainly be expected to provide a notable contribution.

The generation of electric power using wind energy is economically viable today in the windy parts of the world, the economics mainly depending on how the social costs of other forms of power generation are accounted for. Very good prospects exist for improving the economics and the applicability: wind energy technology is maturing in the meantime, and the wind energy option has become part of overall energy policies in several countries.

Wind energy's promising position is the result of research and development activities in many countries extending over the last 10 to 15 years aimed at harnessing an old source of energy with modern methods. Many disciplines have contributed, including physics. We shall outline the physics involved in wind energy systems and discuss what might be called the physical approach to handling some of the problems. It is aimed at the same time to summarise the state-of-the-art and the directions of current developments. There exist a few general textbooks on wind energy, and interested readers can only be referred to two German texts [1, 2] and one in English [3].

Wind power can be exploited in developing countries for pumping water, while applications involving electric power generation are often in a stand-alone fashion for isolated communities, mostly in conjunction with local back-up power such as a diesel generator. Here, however, we shall concentrate on the most advanced application of wind energy, namely the relatively large-scale generation of electric power to feed a public supply grid. Several different forms forms of wind turbine exist but only the familiar "propeller"-type machine (Fig. 1) — the horizontal axis wind turbine — will be considered in demonstrating principles. It is common practice these days to build such machines together in clusters called wind farms or wind parks. Moreover, several thousands of megawatts of wind power have now been installed worldwide.

Converting Energy

A wind energy conversion system essentially comprises: an atmosphere carrying kinetic energy in both ordered and disordered (*i.e.*, turbulent) flow; a rotor to convert in a well controlled manner part of the kinetic energy into mechanical energy of rotation by exploiting the unique properties of airfoils; a transmission system to concentrate the mechanical power into a form suitable for electricity generation; the electricity conversion system (*i.e.*, the generator connected to a grid); a yawing system to direct the rotor to the wind during normal operation; a support system (foundations, tower, nacelle) for the various components; and controls to optimise power production during operation in the safest possible way.

Betz limit

Consider first the conversion of wind flow into mechanical energy. All of the wind's kinetic energy cannot be converted into mechanical power. Flow would have to be stopped completely for full conversion; but no power extraction is possible at zero flow. So the efficiency of power conversion C_p must be zero at flow reductions of 0 and 100%. There should be an optimum at some intermediate value of the flow reduction, which is easily calculated for incompressible and inviscid air flow from the laws of conservation of mass, momentum and energy without specifying how the power is extracted. The derivation is usually attributed to Betz (1920) although the identical result had already been obtained by Lancaster in 1915. According to Betz, the wind turbine is represented as a thin, transparent circular disc (the "actuator disc") of cross-section A interacting with the flow. The stream tube through the disc is is sketched in Fig. 2 where the upstream (undisturbed) wind velocity U is reduced to U' at the disc and to U_∞ far downstream. The force F of the disc on the fluid is equal to the change of momentum $m(U-U_\infty)$ where m is the mass of air passing the disc per unit time. The energy loss per unit time, $m(U^2-U_\infty^2)/2$ equals $U'm(U-U_\infty)$, the work done per unit time by the force F. From this equality follows the remarkable relation

$$U' = (U + U_\infty)/2. \qquad (1)$$

As $m = \rho U'A$ for an air density ρ, the power P is given by

$$P = \rho A(U + U_\infty)(U^2 - U_\infty^2)/4. \qquad (2)$$

It is easily shown that the power extraction is a maximum for $U_\infty = U/3$ whereupon the output power is 16/27 (*i.e.*, about 59%) of the power in the undisturbed flow through an area A, which is $P_{wind} = \rho U^3 A/2$.

The maximum possible value of C_p = 16/27 is known as the Betz limit. The velocity reductions are often expressed in an induction factor a so that $U' = U(1-a)$ with a = 1/3 at the optimum condition.

The Betz result is not without its limitations. The fundamental relation (Eq. 1) follows directly from Fig. 2. However, the edge of the actuator disc leads to a singularity in the flow. The streamline through the edge

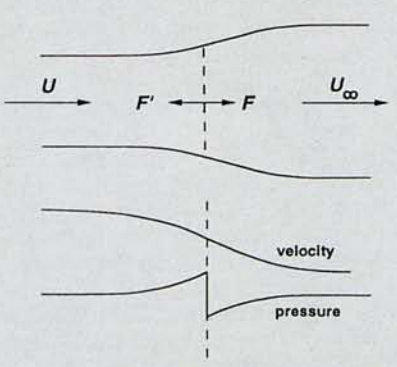

Fig. 2 — Representation of flow through an idealised wind turbine. a, upper) Air initially at a velocity U flows in a stream tube across a thin, transparent circular disc, whereupon the tube expands and the velocity is reduced far downstream to U_∞; a force F is exerted on the disc. b, lower) The corresponding variation of air velocity and pressure along the axis of the tube.

Professor J.B. Dragt was appointed in 1989 to a new chair for wind energy at the Delft University of Technology, where he heads the Institute for Wind Energy. After studying physics at the Free University , Amsterdam, he joined the Reactor Centre of The Netherlands in 1960, receiving a Ph.D. in 1968 for nuclear reactor noise analysis. Professor Dragt promoted the modern development of wind energy technology, and he is presently serving as the Vice-Chairman of the European Wind Energy Association.

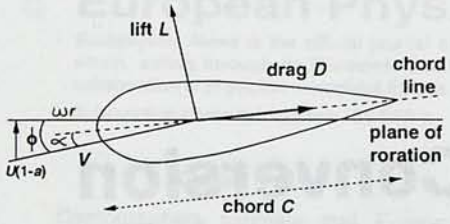

Fig. 3 — Inflow conditions at a wind turbine blade in the plane perpendicular to the span. Lift (L) and drag (D) forces are generated by air at an effective velocity V striking the blade at an effective angle α. The air velocity over the plane of the rotor is U' and φ defines the flow angles along the blade.

should in fact resemble a logarithmic spiral winding up towards the disc edge, and unwinding in the downwind direction. So even the simple disc model leads to a very interesting flow problem: there are singularities in the forces between flow and disk at the edge and Eq. 1 may be slightly violated, with the real power extraction being somewhat higher than the Betz limit, at least theoretically speaking [4].

Power extraction

There are several possibilities for realising a practical device to convert power according to the theoretical principles outlined above. Fig. 3 illustrates a cross-section perpendicular to the span of the rotor blade of the familiar horizontal axis wind turbine. The effective wind speed is seen to result from the perturbed wind speed U' and the movement of the blade. The effective wind with a velocity V is incident upon the blade at an angle α, which results in the aerodynamic forces at a distance r from the axis on an annulus of width dr of:

$$dL = \rho V^2 c C_l(\alpha) dr/2 \qquad (3a)$$

$$dD = \rho V^2 c C_d(\alpha) dr/2 \qquad (3b)$$

for lift and drag, respectively. The coefficients C_l and C_d depend on the shape of the airfoil profile which is chosen (*e.g.*, Fig. 4 giving examples of measured values of C_l and C_d for a particular profile) and c is the blade's chord length. The resulting component of lift and drag in the direction of the motion is the driving force of the rotor so one clearly requires $C_l >> C_d$.

The unknown parameter in Fig. 3 is the induction parameter a that is a measure of the extent to which the wind velocity is decreased. To estimate this parameter, consider the lift generated by the vortex built up around the blade and bound to the blade. The circulation of this vortex per unit blade length is $dL/\rho V$, where the circulation is defined as the line integral of the tangential velocity component along a closed curve (it is a measure of the enclosed vorticity). Outside the blade's boundary layer, flow is taken to be irrational, *i.e.*, vorticity is conserved so sheets of vorticity must be flowing off the rear edge of the blade to compensate for radial changes in circulation. In particular, a vortex must be released at the tip of each blade. These tip vortices will be spiralling in the wake of the rotor in the same way as the wiring of an electrical solenoid (see cover illustration). The velocities generated by such a coil of vorticity obey the same law of Biot and Savart as the magnetic inductions of an electric coil. From this analogy one can understand that for a densely wound coil (*i.e.*, small incident angle ϕ in Fig. 3), the induced velocity at the rotor plane (*i.e.*, at the entrance to the solenoid) is one-half the value far into the coil. This estimate gives the same result as Eq. 1 so the analogy agrees with the simple model.

The actual situation is more complicated: vortices are free, so apart from winding up there will also be expansion due to repulsion between the vortices — an expansion corresponding to the flow expansion shown in Fig. 1. The vortex pattern depends on the bound vortices of the blades, and thus on their lift, but the lift depends on the induction factors and thus on the free vortex structure in the wake. Accurate calculations therefore involve iteration.

Design calculation

The process clearly defines a complicated, but physically interesting, problem. Several efforts based on various approximations have been made to compute the velocity field of the wake, but a satisfactory rotor design method has not been forthcoming up to now. A much simpler approach is adopted for design purposes: the induction factor a is estimated from a momentum conservation calculation similar to the Betz model, where the aerodynamics of the blade is smeared out over the azimuth angles (so it effectively assumes an infinite number of blades). This approach has been reasonable successful for stationary conditions.

Sweeping the Wind

The rotor efficiency is often expressed as a function of the dimensionless parameter $\lambda = \omega R/U$ giving the tip speed ratio for an angular speed of rotation ω for a tip radius R. It is this quantity that determines the flow angles ϕ between the effective incident wind speed and the rotor plane (see Fig. 3) along the blade. The function $C_p(\lambda)$ for a given rotor, calculated in the manner outlined above, typically increases to a maximum at a certain λ_{opt} (called the design tip speed ratio) on increasing λ, and then decreases more sharply.

When designing a rotor, the first thing one must do is select a suitable value for λ_{opt}. A fairly high value is often recommended (say >6) since the loss of power associated with rotation of the wake owing to the conservation of angular momentum is not accounted for in the Betz model. For a given power, the rotor's angular momentum, and therefore this loss, is smaller the higher the speed of the rotor, and thus λ_{opt}.

One also seeks the lowest possible profile drag, *i.e.*, for a chosen, the angle of incidence along the entire blade should be the angle corresponding to where C_l/C_d is a maximum (about 10° for the profile described by Fig. 4c). This means that the blade must be twisted, with the twist decreasing from the root of the blade towards the tip, in theory in a hyperbolic manner, but in practice usually linearised. For a twisted blade, one should maintain the corresponding value of C_l (≈ 0.8 for the example of Fig. 4) along the whole blade. The significance of this requirement is seen by comparing Eq. 3b for the rotor drag for an annulus of width dr (after multiplication by the number of blades B) with the momentum change similar to that calculated for the Betz model. This leads to the condition

$$c = 8\pi a(1-a)R^2/BC^2_{l,opt}\,\lambda^2_{opt} r$$

so the chord length should decrease towards the tip (again hyperbolically, but usually linearised for practical reasons). Moreover, for high λ_{opt}, the blade should be very slender. Note, however, that the requirement on C_l/C_d becomes very severe for a highly efficient rotor of this sort.

The present trend in rotor design is therefore to build slender and twisted rotors with a small number of slender blades with decreasing chords towards the tips, operating as a high-speed rotor, and using airfoils with large lift-to-drag ratios. This is contrary to intuition, which favours a large number of blades and large chords. Harvesting wind power thus appears to show a very interesting feature in that while the blades of a turbine cover only a small part of the total rotor area, a large proportion of the kinetic energy through the area may be swept up. This unique broom-like, material-saving property is a direct consequence of the use of the lift force to drive the machine. However, the Betz limit of 59% is not reached in practice as modern rotors have efficiencies of around 45%.

Coping with Turbulence

One of the most important aspects of designing wind turbines is to make the machines strong enough to withstand fluc-

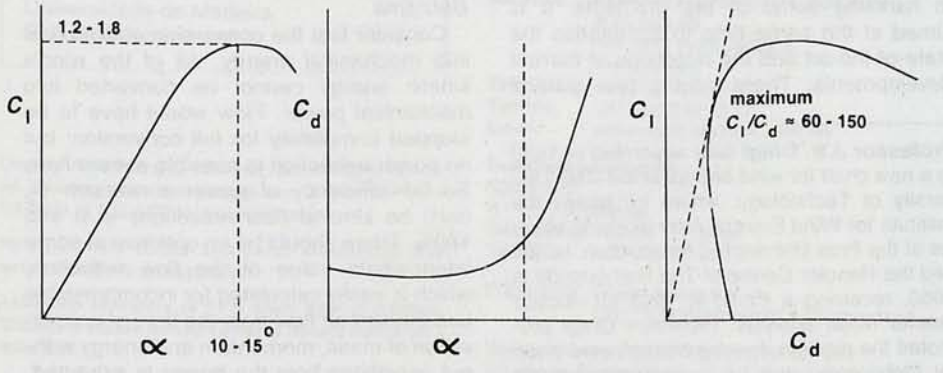

Fig. 4 — Examples of variations of lift and drag coefficients C_l (a, left) and C_d (b, middle) as a function of the effective angle. (c, right) Optimal driving requires C_l/C_d to be a maximum.

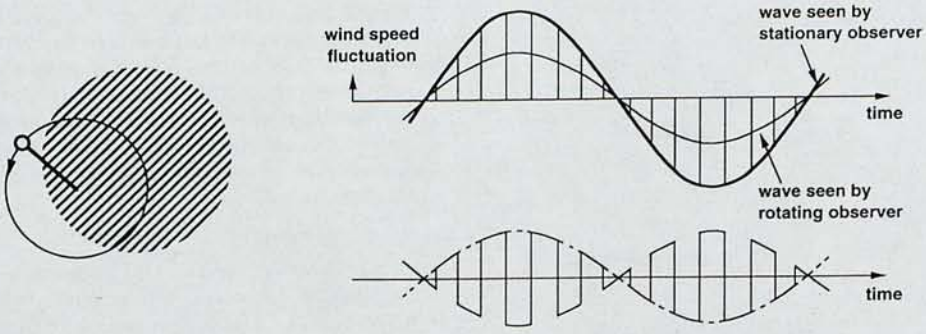

Fig. 5 — The effect of the finite spatial structure of turbulent wind. a, left) Schematic of the path of a rotor blade element (circle) through a turbulence bubble (hatched). b, upper right) Transformation of the wind velocity fluctuation pattern for a rotating observer. An observer sitting on the rotor blade sees a square-wave fluctuation in the longitudinal wind speed that is modulated by the turbulence wave. c, lower right) The same pattern after removal of the direct turbulence component.

tuating wind loads that lead in the long term to fatigue damage. Rotor loading due to turbulence is an example of one aspect particular to wind turbines that is not standard practice in aerodynamic engineering. This loading was initially accounted for by considering temporal variations, but from 1983 it was realised that spatial variations of wind speed over the rotor area are at least as important. These spatial variations are transformed into time variations of the wind felt by the rotor.

Frequency shifts

The rate of change of the turbulent wind field is fairly slow (time constant of the order of 0.1 s) with respect to the rate of rotation of a rotor (about one revolution per second). If a blade meets a certain pattern of wind speed fluctuations (or corresponding load fluctuations) on its path during one revolution, it will meet a similar, and only slightly modified pattern during the next revolution, and so on. The frequency spectrum of wind speed (or load) fluctuation will thus show components at the frequency of rotation and at its harmonics.

For a more quantitative view, consider an observer at a point on a blade rotating at a frequency f_0 through the turbulent field. The atmospheric turbulence can be thought of as comprising contributions from many different frequencies among which we consider a frequency f with $f < f_0$. The finite spatial structure is accounted for by considering this wave to be incident over a finite area, hatched in Fig. 5a. Our observer will only look at the longitudinal variations in wind velocity as these are the most relevant for determining blade forces. Diving in and out of a turbulence bubble, the observer experiences a (square) wave of frequency f_0 modulated by the turbulence wave of frequency f (see Fig. 5b).

Regarding the frequency content of this signal: we still have the original turbulence wave but it is attenuated (Fig. 5b). Superimposed on it is a wave modulated according to Fig. 5c composed of side-band frequencies f_0+f and f_0-f, together with frequencies $2f_0 \pm f$, $3f_0 \pm f$, *etc.* due to the non-sinusoidal carrier wave. The result of the frequency shifts is that the usual turbulence spectrum for a stationary observer is transformed (see Fig. 6a) whereby part of the original spectral component $S(f)$ is filtered to $k_0 S(f)$, with increasing attenuation at increasing frequencies since higher frequencies correspond to smaller turbulence bubbles. The fluctuating power filtered away is meanwhile displaced to peaks in the vicinity of the rotation frequency f_0 and its harmonics. The shape of the filter-like functions $k_0(f)$, $k_1(f)$, $k_2(f)$,.... is determined by the spatial structure of the turbulence, *i.e.*, by the coherence of simultaneous fluctuations of the longitudinal wind speed at any pair of points in the rotor plane.

This is, of course, a very approximate picture. Mathematically rigourous treatments can be developed in several different ways, either in the time domain (based on correlation functions) or in the frequency domain (spectral density and coherence functions). Consider, as a example, the latter [5]. One can show that the auto-spectral density function of the fluctuations for the rotating observer is simply

$$S_{rot}(f) = K_n(| f - nf_o |)$$

where K_n are the Fourier coefficients of the cross-spectral density function in non-rotating coordinates. Fig. 6b gives an example of the spectrum calculated using this formula assuming a semi-empirical coherence function which is exponential in both frequency and the (linear) distance (other models assume isotropic turbulence). The power spectrum for the stationary observer is seen to be shifted for the rotating observer to give pronounced peaks in the power density at high frequencies.

We actually need, of course, the spectra and cross spectra for many points on the blades. The transformation formula given above remains valid provided $S_{rot}(f)$ is taken to be a matrix of spectra for pairs of points on a rotor.

Fatigue

The shift of the fluctuating power from low to high frequencies is very relevant for fatigue loading, so the effects must be taken into account in design calculations. Engineering practice has up to now carried out the calculations for irregular loads in the time domain. Special algorithms have been developed (in particular, "rain-flow counting") to select from the time-domain load pattern the load cycles that are relevant for fatigue damage. Acceptable methods based on stochastic models for fatigue assessment — highly desirable for the turbulence loads — are still lacking, although some promising ideas have been launched.

Assuring Adjustability

Anyone interested in wind energy will quickly notice that the machines grow larger and larger. Ten years ago, a 16 m diameter, 50 kW nominal power machine was fashionable whereas rotors with diameters of 30-50 m and powers corresponding to 0.5-1.0 MW per unit are nowadays on the market. Bigger machines have some advantages: being tall they better capture the wind and being more powerful they make the infrastructure of

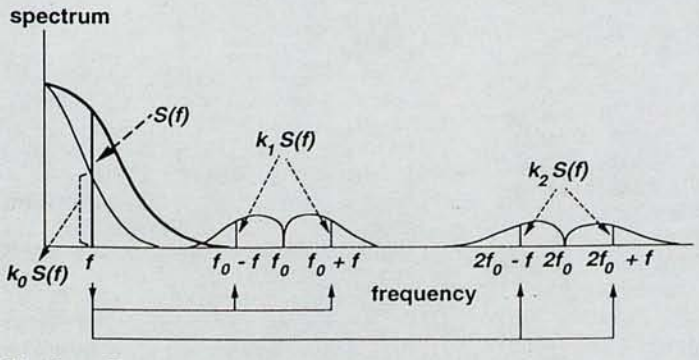

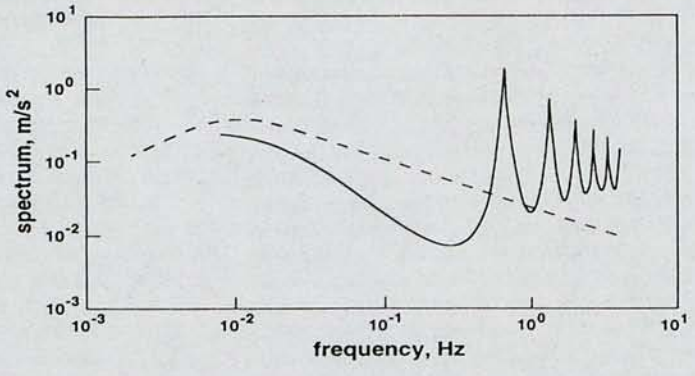

Fig. 6 — Transformation of the longitudinal wind velocity fluctuation spectrum for a stationary observer (thick line) into the spectrum for a rotating observer (thin line). a, left) Part of the original spectral component S(f) is filtered to $k_0 S(f)$ and the fluctuating power filtered away is displaced into peaks centred around the rotation frequency f_0 and its harmonics. The shapes of the filter-like functions $k_0(f)$, $k_1(f)$,... are determined by the coherence between simultaneous fluctuations in the wind velocity at pairs of points in the rotor plane. b, right) Spectra, calculated assuming an exponential coherence function, for a stationary observer and for rotational sampling.

wind farms simpler. But there are limits to the increase in size: energy capture increases as the square of the rotor diameter but the mass (determinant for cost) increase roughly as the cube of linear dimensions. The thickness of material is largely determined by the many types of dynamic loads. Some are deterministic (*e.g.*, those due to gravity or to gradients in the wind speed in a vertical direction) while others are stochastic (*e.g.*, due to turbulence). An obvious way to better cope with the dynamic loads is to make the construction more flexible so as to overcome the square-cube limitation [6].

Flexibility can be introduced in a variety of ways. Following developments in helicopter design, the rotors may be flexible. For instance, two-bladed rotors may use a teetering hub (a device that allows counteracting flap motions of both blades) to suppress bending moments in the hub owing to unequal loading of the blades. Blades may also be hinged individually to avoid bending moments at the blade root (Fig. 7). One can use both normal hinges as well as flexible elements made from deformable materials such as elastomers. The blade will try to dynamically adjust the flap angle β in Fig. 7 so that the resultant of the centrifugal and aerodynamic forces acts along the span of the blade (bending stresses cannot arise at the hinge).

Other forms of flexibility can be envisaged (in the drive train or in the conversion control system, for instance) that allow power fluctuations to be stored either in rotor inertia, instead of being transferred to the conversion system, or in the turbine tower or the foundations.

Instabilities

Modern development trends apply one or more forms of adjustability to provide more cost-effective and long-lasting machines. However, a generic problem is associated with this approach. It arises because there are many possible vibration modes for the overall system, coupled in several ways, often with eigenfrequencies which depend on the rotor speed. It is well known that instabilities may develop if eigenfrequencies of coupled modes come close together (a famous example is classical blade flutter, where flap and torsion motions of a blade, wing or bridge deck interact in a catastrophic manner). Instabilities may also result from coupled blade motions and tower torsion (the overall effect is similar to the "ground resonance" in helicopters).

A careful dynamic analysis is required [7] and it is common practice to start from the Lagrange equations for the generalised coordinates of the system and its derivatives. The resulting (non-linear) equations of motion are integrated numerically. Generalised momenta are used occasionally [8] for higher computational efficiency. Most potential instabilities, including the ones mentioned above, can be studied by linearising the equations. A non-linear analysis of the type illustrated in the next section is often performed as well.

Power Control and Stability

Several parameters of a wind turbine have to be controlled (*e.g.*, yaw control tries

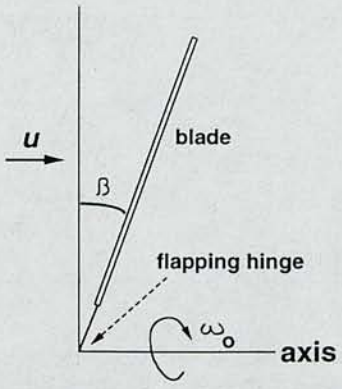

Fig. 7 — An illustration of a hinged (or flapping) rotor blade that avoids bending at the root. The blade dynamically adjusts the flap angle β so that the resultant of centrifugal and aerodynamic forces acts along the blade. Stalling may induce vibrations (see text).

to keep the rotor perpendicular to the wind). We shall concentrate on power control which aims to limit the power of the generator to a maximum value called the rated power P_{rated}. A wind turbine has to be designed for a maximum power level and loads, so the efficiency of the rotor must be decreased above a certain wind speed U_{rated} (typically 12 m/s) corresponding to P_{rated}. Full capture of the power of the wind at high powers (increasing as U^3 according to Eq. 2) above wind speeds of U_{rated} is not justified economically.

Two techniques are used to control the power. Pitch control involves pitching the blades (reducing the angle α in Fig. 3) by turning the whole blade so that C_l is reduced. The other technique is mechanically simpler. It involves increasing the angle α to above 10-15° to reduce C_l to bring about flow separation (see Fig. 4) called stall. One sees from Fig. 3 that an increasing wind velocity also increases the angle of incidence at a constant rotor speed. It is possible to design the rotor so that the corresponding decrease in C_l (together with some increase in C_d) keeps the power fairly constant above U_{rated} up to a high value of the wind speed (around 20 m/s), at which point the rotor must be stopped. The rotor must be kept at a nearly constant speed for stall control. This can be conveniently achieved using an induction generator connected directly to the grid so that the mains frequency fixes the rotor speed.

Stall-induced vibration

If the blades flex in the direction of the wind (flap direction), there is a potential hazard in this attractive method of control based on adjusting stall. Decreasing lift with increasing velocity may (depending on the design) lead to a negative gradient of the moment of the axial force driving the flap motion. Suppose a rotor is in the negative gradient range and a blade happens to move in the direction of the wind. The blade will then experience a lower than average wind velocity and an increased flap moment. The motion is thereby amplified and the blade becomes unstable. This situation is easily studied for the freely hinged blade of Fig. 7 where the moment of inertia with respect to the hinge is denoted by I. We balance moments and approximate the oscillatory motion with non-linear damping about the operating point in terms of a third-order polynomial. There is an operating condition with respect to the equilibrium value of the flap angle β for which the flap velocity $x = \dot{\beta}$ satisfies the equation

$$I\ddot{x} - \mu(1 - cx^2)\dot{x} + I\omega_0^2 x = 0$$

with constants μ and c. This is nothing but the famous Van der Pol equation. Few equations have been investigated in more detail. A characteristic of its solution is limit cycle behaviour, *i.e.*, the generation of spontaneous periodic oscillations. In the case of wind turbines at stall, phenomena have been observed which may be explained by this type of self-excitation ("stall-induced vibrations") [9].

Complications

The wind turbine is in reality more complex than the simple model just described. The wind speed U is highly variable and stochastic (see above); aerodynamics at stall is not as simple as described by Eqs. 3; three-dimensional flow around the blade can be important; and aerodynamic forces tend to exhibit hysteresis. Further studies of these poorly understood features are needed. Formulations based on empirical models combined with dynamic rotor models allow analyses of complicated, but very interesting, non-linear dynamics. Such investigations are very relevant for the application of wind turbines as the prediction of instabilities (or rather, the proof of stable behaviour) is essential for estimating fatigue life.

Conclusions

Some issues involved in designing wind turbines for large-scale power generation shows the important rôle played by physics and physical understanding in the technical development of modern devices. Physics (and physicists) may be expected to continue to help tackle several aspects which call for further attention, notably stochastic fatigue and the effects of details of wind flow (highly variable speed, three-dimensional flow) and hysteresis on the dynamic stability of rotors. In general, however, wind energy technology has matured, making it a valuable contributor to solutions to urgent environmental problems.

[1] Hau E., *Windkraftanlagen* (Springer-Verlag) 1988.
[2] Molly J.P., *Wind Energie: Theorie, Anwendung, Messung* (Verlag C.F. Müller, Karlsruhe, Germany) 2nd Ed., 1990.
[3] Freris L.L., *Wind Energy Conversion Systems* (Prentice Hall, New York) 1990.
[4] Kuik, G.A.M. van, *Proc. European Wind Energy Conf.*, Glasgow, UK (1989) 158.
[5] Dragt J.B., *Proc. EC Wind Energy Conf.*, Madrid (1990) 274.
[6] Snel H., *et al.*, *ibid.*, p. 428.
[7] Eggleston D.M. and Stoddard F.S., *Wind Turbine Engineering Design* (Van Nostrand, New York) 1987.
[8] Holten Th. van, *Proc. 13th European Rotorcraft Forum*, Arles, France (1987), No. 6.8.
[9] Lundsager J.P., *et al.*, *Risø National Lab. Report* M-2253 (1981).